Photoinduced Electron Transfer in a Tris(2,2′-bipyridine)-C_{60}-ruthenium(II) Dyad: Evidence of Charge Recombination to a Fullerene Excited State**

Michele Maggini,* Dirk M. Guldi,* Simonetta Mondini, Gianfranco Scorrano, Francesco Paolucci,* Paola Ceroni, and Sergio Roffia

Abstract: A 1,3-dipolar cycloaddition reaction of azomethine ylides to C_{60} has been used to prepare a fulleropyrrolidine covalently linked to a substituted tris(2,2′bipyridine)ruthenium(II) chromophore. Electrochemical studies revealed a single one-electron reversible oxidation of the ruthenium center and ten one-electron reversible reductions, five of them occurring at the C_{60} core and five at the bipyridine (bpy) ligands. Steady-state fluorescence and time-resolved flash-photolytic investigations of dyad **6** are reported in solvents of different polarity. The emission in toluene/CH_2Cl_2, CH_2Cl_2, and CH_3CN was substantially quenched, relative to model complex **8**, suggesting intramolecular quenching of the ruthenium MLCT excited state. Picosecond-resolved photolysis of **6** showed light-induced formation of the photoexcited ruthenium center, which undergoes rapid intramolecular electron transfer. Nanosecond-resolved photolysis revealed a charge-separated state ($\tau_{1/2} = 210$ ns in CH_2Cl_2 and $\tau_{1/2} = 100$ ns in CH_3CN) that decays to the ground state by regeneration of the ruthenium MLCT excited state in CH_2Cl_2 or through the formation of the C_{60} triplet excited state in CH_3CN.

Keywords: cyclic voltammetry · dyad · electron transfer · fullerenes · ruthenium

Introduction

Photoinduced electron transfer in covalently linked donor-bridge-acceptor molecular systems has been extensively studied to exploit the potential ability of nonbiological systems to transform and store optical energy.[1] Factors such as structure and distance between donor–acceptor (D–A), nature and polarity of the solvent, temperature, free energy changes, and charge recombination have been systematically modified in order to control charge-separation dynamics and efficiencies.[2] The ultimate motivation of these studies is to make use of the long-lived charge-separated (CS) state in artificial photosynthesis or specific interactions with external physical or chemical phenomena.

[*] Dr. M. Maggini, Dr. S. Mondini, Prof. G. Scorrano
Centro Meccanismi Reazioni Organiche-CNR
Dipartimento di Chimica Organica
Via Marzolo 1, I-35131 Padova (Italy)
Fax: (+390) 49-8275239
E-mail: maggini@chor02.chor.unipd.it
Dr. D. M. Guldi
Radiation Laboratory, University of Notre Dame, Indiana (USA)
Dr. F. Paolucci, Dr. P. Ceroni, Prof. S. Roffia
Dipartimento di Chimica G. Ciamician, Università di Bologna (Italy)

[**] Supporting information for this contribution is available on the WWW under http://www.wiley-vch.de/home/chemistry/, or directly from the author.

[60]Fullerene, the most popular representative of the fullerene family, has emerged as an important molecular unit in light-triggered electron-transfer (ET) reactions owing to its remarkable electron-acceptor properties upon photoexcitation.[3] In addition, the electronic-absorption properties of $C_{60}^{\bullet-}$, which are substantially different from those of neutral C_{60}, allow an accurate analysis of ET dynamics in C_{60}-based D–A assemblies.[4] The rapid progress of fullerene chemistry[5, 6] has promoted the covalent linking of a wide variety of electron-rich groups to C_{60}, and numerous dyads have been produced and studied in light-triggered ET reactions.[6, 4a]

In this context, we have recently examined the photophysical properties of a D-bridge-A system based on a functionalized fulleropyrrolidine[7] covalently attached to a substituted tris(2,2′bipyridine)ruthenium(II)[8] chromophore ($[Ru(bpy)_3]^{2+}$) through a flexible triethylene glycol chain.[9] As a thin solid film, this dyad undergoes photoinduced electron transfer to give the Ru^{3+}–$C_{60}^{\bullet-}$ CS state with a lifetime on the order of milliseconds at 80 K.[10] Photolysis in polar solvents confirmed a long-lived radical-pair generation, which is hampered in nonpolar media by very fast back electron transfer. We report in this paper on the synthesis, electrochemistry, and photophysical behavior of a Ru^{2+}–C_{60} dyad in which the flexible spacer has been replaced by a rigid androstane skeleton; this should prevent conformational changes in the ground and excited states. In contrast to the flexible dyad, direct evidence of a relatively long-lived CS

  0947-6539/98/0410-1992 $ 17.50+.50/0

state is given also in nonpolar solvents by the characteristic fullerene radical-anion band at $\lambda_{max} = 1040$ nm. More interestingly, in CH_3CN back electron transfer yields the C_{60} triplet excited state rather than a recombination to the molecular ground state, which is observed in CH_2Cl_2.

Results and Discussion

Synthesis: Our synthetic approach towards a fullerene-based photoactive dyad relies upon the 1,3-dipolar cycloaddition of azomethine ylides to C_{60}.[7] The initial step in the synthesis of derivative **6** is the coupling of 2,2′-bipyridine-5-carboxylic acid (**2**; from bpy **1;** Scheme 1) to commercially available androstanone alcohol **3** (4,5-dihydrotestosterone) under standard conditions (DCC/DMAP).

The resulting ester-ketone **4** was condensed with sarcosine in the presence of C_{60} to afford fulleropyrrolidine **5** in 19% isolated yield (65% based on unreacted C_{60}). Addition of the enantiopure derivative **4** to C_{60}, by azomethine ylide cycloaddition, generates a new stereocenter in position 2 of the pyrrolidine ring. As a consequence, **5** is expected to be a diastereomeric mixture. A careful analysis of the proton spectrum revealed that derivative **5** is in fact a mixture of two diastereoisomers in about 3:1 ratio, calculated by integrating the respective resonances of the methyl groups in the spacer.

Dyad **6** was synthesized by coordinating ligand **5** to ruthenium, through refluxing $Ru(bpy)_2Cl_2 \cdot 2H_2O$ and **5** in 1,2-dichloroethane in the presence of excess NH_4PF_6. The use of an ammonium salt promotes chloride displacement by ligand **5** in the $Ru(bpy)_2Cl_2$ complex, making the formation of dyad **6** faster. The reaction was monitored by TLC (toluene/AcOEt), following the disappearance of **5**. After filtration, the solution was concentrated under reduced pressure, and the brownish solid was washed with toluene, MeOH, and water to remove unreacted **5**, $Ru(bpy)_2Cl_2$, and excess NH_4PF_6, respectively. The solid residue was then dissolved in THF, filtered, and after evaporation of the solvent, dried in vacuo to afford compound **6** in 41% yield. Compound **6** is reasonably soluble in methylene chloride, 1,2-DCE, and CH_3CN, but is insoluble in toluene. It was characterized by ^1H and ^{13}C NMR techniques (see supporting information), optical spectroscopy, electrochemical techniques (vide infra), and elemental analysis. The APCI mass spectrum shows a cluster of signals with a maximum at 815 *m/z* corresponding to the expected mass for the ionic species $[(M^{2+})/2]$.

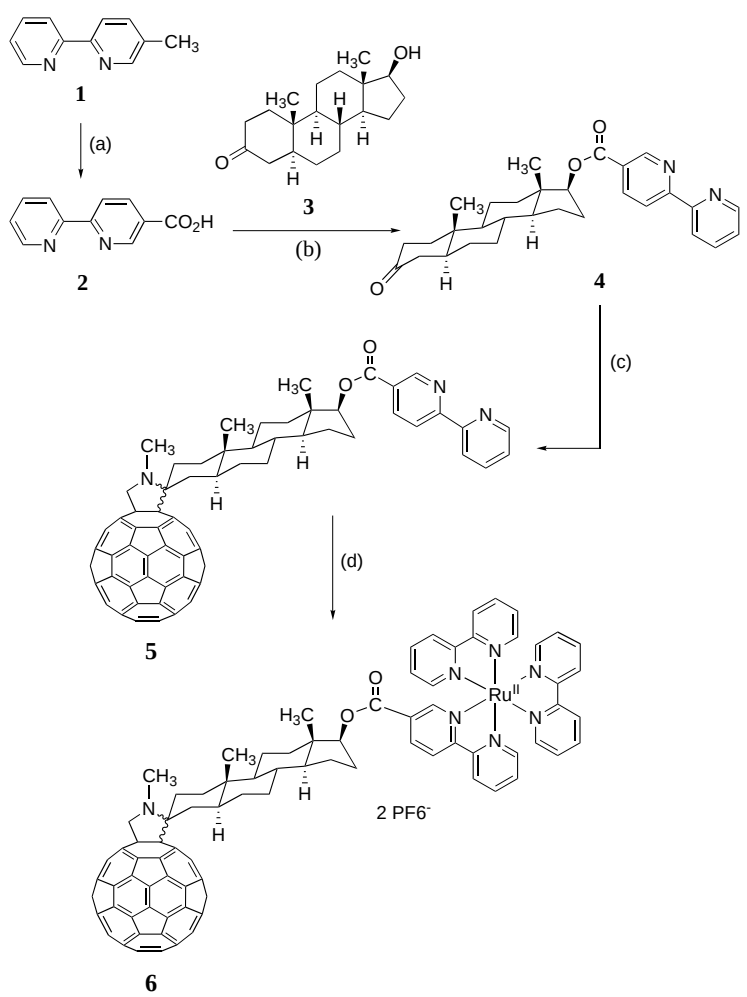

Scheme 1. Synthesis of dyad **6**. Reagents and conditions: a) Ref. [29]. b) DCC/DMAP, CH_2Cl_2, 20 h, 65%. c) *N*-Methylglycine, C_{60}, toluene, reflux, 2.5 h, 65%. d) $Ru(bpy)_2Cl_2 \cdot 2H_2O$, NH_4PF_6, DCE, reflux, 9h, 41%.

The use of a diastereoisomeric mixture of ligand **5** to bind Ru^{II} could in principle constitute a complication to the correct photophysical characterization of the final C_{60}-based ruthenium dyad, since diastereoisomers have different spatial orientations that may influence properties such as rate of energy or electron transfer. Molecular-mechanics calculations have been performed to derive the minimum-energy structure of the diastereoisomers of ligand **5**, and to determine the edge-to-edge distance between the bpy and C_{60} moieties. A set of different conformations for each diastereoisomer was obtained from MM2 calculations; each conformer differs from the next by a 60 degree individual rotation of the three single bonds of the ester function that links androstane to bpy. The most stable conformer in each set was re-optimized at the PM3 semiempirical level. It has been found that the edge-to-edge distance between bpy and C_{60}, in the minimized conformations, does not differ substantially in the two diastereoisomers (11 vs. 12 Å). As a consequence, we would expect that the corresponding isomeric mixture of dyad **6** to exhibit a similar photophysical behavior compared with that of each diastereoisomer.[11] To confirm this hypothesis, small amounts of the two pure diastereoisomers of ligand **5** were obtained by subjecting the isomeric mixture to HPLC. Coordination to ruthenium gave the corresponding dyads, which were separately tested in photophysical experiments. It was found that these dyads behave essentially like the mixture. For the sake of simplicity, and to avoid redundancy, all the experiments described throughout this paper were performed on the mixture of diastereoisomers of dyad **6**.

Derivatives **7**[7a] and **8** (Scheme 2) were synthesized and used as model compounds, together with androstanone-bpy **4** and the C_{60}-based ligand **5**, in the electrochemical and photophysical characterization of dyad **6**.

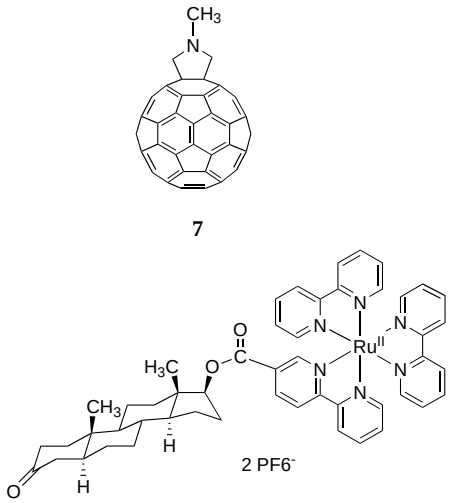

Scheme 2. Schematic daigram of the structures of **7** and **8**.

Electrochemistry: Figure 1 shows the cyclic voltammetric (CV) curves (a and b), the differential pulse voltammetric (DPV) curve (c) for 3.0×10^{-4} M CH_3CN (a) and THF (b, c) solutions of dyad **6** at $T = 25\,^{\circ}C$, and the simulated CV curve of **6** (d).

In the region of positive potentials, a single reversible diffusion-controlled one-electron oxidation process is observed with $E_{1/2} = +1.34$ V. This process can be confidently attributed to the metal-centered $Ru^{II} \rightarrow Ru^{III}$ oxidation on the basis of the number of electrons exchanged and of similarity of its $E_{1/2}$ with that for the oxidation of $[Ru(bpy)_3]^{2+}$ in CH_3CN (+1.29 V).[8b] The 50 mV positive shift of the $E_{1/2}$ value in the case of the dyad **6** can be explained in terms of the presence of the electron-withdrawing carboxy group on one of the bpy ligands.[12]

The pattern of the curves in the cathodic region is more complex due to the presence of several reduction processes. However, reliable information on the number and nature of these processes can be derived from a careful analysis of the curves. In particular, the morphology of CV and DPV curves, the independence on the sweep rate of the current function, and the simulation of CV curves indicate that the observed processes can be described as ten successive one-electron, diffusion-controlled, reversible reduction steps. The simulated CV curve, carried out according to procedures previously described[13] under the conditions of Figure 1b, is reported in Figure 1d; the agreement between the experimental and simulated curves is satisfactory. The values of $E_{1/2}$ for the various steps are reported in Table 1; these were obtained from CV curves as a mean of the cathodic and anodic peak potentials for single peaks, and by means of the simulation for the doublets.

In order to identify the redox sites, and to obtain information on their mutual interactions, the electrochemical behavior of **6** has been compared with that of derivatives **4**, **5**, **7**, and **8** (Schemes 1 and 2). These derivatives represent good models of increasing complexity for the various parts of the dyad. All compounds show reversible diffusion-controlled processes (see supporting information). The $E_{1/2}$ values for the various reduction steps, deduced as previously described, are collected in Table 1 and are displayed, together with those relative to **6**, in the genetic diagram shown in Figure 2.

The reduction of fulleropyrrolidine **7** gives rise to five one-electron processes.[14] In compound **5**, which contains the substituted bpy ligand in addition to the fullerene moiety, the third and fourth processes become two-

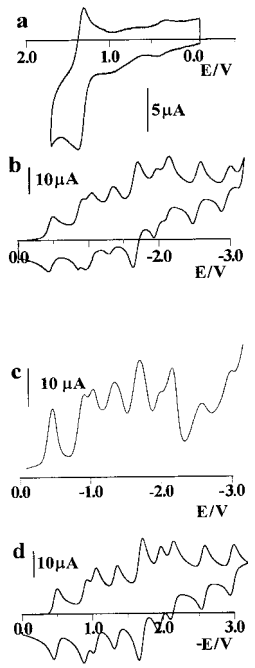

Figure 1. a) CV curve of **6** (0.3 mM) in CH_3CN solution (0.05 M TBAH); b) CV curve of **6** (0.3 mM) in THF solution (0.05 M TBAH); c) DPV curve of **6** (0.3 mM) in THF solution (0.05 M TBAH). Working electrode = Pt, $T = 25\,^{\circ}C$, sweep rate 0.2 V/s. d) Simulated CV curve of **6** under the conditions of b).

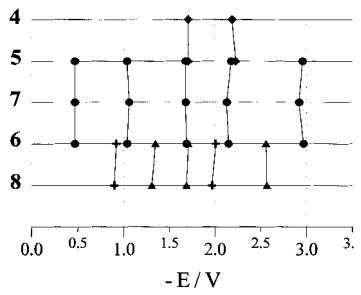

Figure 2. Comparison of $E_{1/2}$ values (genetic diagram) for compounds **4**–**8**.

Table 1. $E_{1/2}$ values (V vs SCE) of the redox couples of dyad **6** and derivatives **4**, **5**, **7**, and **8**, detected by CV (sweep rate = 0.2 V s^{-1}) in 0.3 mM THF solutions (0.05 M TBAH), at 25° C.[a]

	$Ru^{III/II}$	1	2	3	4	5	6	7	8	9	10
6	+1.34[b]	−0.47 (−0.41)[b,c]	−0.92	−1.04	−1.35	−1.69	−1.71	−1.95	−2.15	−2.56	−2.97
5		−0.47	−1.04	−.168	−1.71	−2.18	−2.23	−2.96			
7		−0.47	−1.06	−1.68	−2.15	−2.96					
8	+1.34[b]	−0.90	−1.31	−1.69	−1.97	−2.57					
4		−1.71	−2.19								

[a] Working electrode: Pt, $E_{1/2}^{Fc+/0} = 0.58$ V (25 °C). [b] CH_3CN (0.05 M TBAH) solutions. [c] Not fully reproducible due to adsorption.

0947-6539/98/0410-1994 $ 17.50+.50/0 *Chem. Eur. J.* **1998**, *4*, No. 10

electron charge transfers. The total number of exchanged electrons is now seven. The comparison with the behavior of model **4** shows that the two-electron peaks recorded for **5** derive from the superimposition of the reductions of the fullerene and substituted bpy moieties. The coincidence of the $E_{1/2}$ values for the reductions in derivative **5** with the corresponding values in models **4** and **7** indicates that the androstane spacer allows practically no mutual interactions between bpy and C_{60}. This means that complex **8** should represent a suitable model for understanding the behavior of the ruthenium moiety in dyad **6**. Derivative **8** exhibits five one-electron reduction processes, one less than the number expected on the basis of the CV behavior of the free ligands (two per bpy unit). Probably, the last process is located outside the accessible potential range. The identification of the redox sites has been performed in analogy to similar heteroleptic ruthenium complexes such as $[Ru(2,3\text{-}dpp)(bpy)_2]^{2+}$ and $[Ru(2,5\text{-}dpp)(bpy)_2]^{2+}$ (2,3- and 2,5-dpp = 2,3- and 2,5-bis(2-pyridil)pyrazine).[15] In these complexes two bpy units are present together with a dpp ligand that, in analogy to **5**, is easier to reduce than the other two ligands. The study of the ligand-based redox series for two families of complexes $[Ru(L)_n(bpy)_{3-n}]^{2+}$ (L = 2,3- or 2,5-dpp; $n = 0, 1, 2, 3$) has shown that the first electron enters into the 2,3-dpp or 2,5-dpp ligand, while the second and third electrons go into each of one of the unsubstituted bpy groups. The next three successive electrons enter in the same sequence coupling to the first ones in the respective redox orbitals. The same succession is proposed for the five electrons introduced into compound **8** as illustrated in Figure 2.

On the basis of the assignment for model compounds **7** and **8**, a satisfactory identification of the redox sites in dyad **6** has been obtained. In particular, from the diagram in Figure 2, the redox pattern of dyad **6** corresponds to the virtual superimposition of those observed for the reduction of the fullerene moiety and of the ligands coordinated to the metal. This confirms that no substantial interaction between the two different electroactive groups occurs through the spacer. Furthermore, comparison between the behavior of dyad **6** with that of compounds **7** and **8** shows that the missing electron, which would make the ligand-based redox series for dyad **6** complete, corresponds to one unsubstituted bpy.

Photophysical measurements

Ground-state absorption spectra: The absorption spectrum of ligand **5** in methylcyclohexane is very similar to those reported earlier for 6,6-closed, monofunctionalized C_{60} derivatives.[16] Bands at around 625, 636, 655, 669, 679, 689, and 701 nm can be distinguished. The latter refers to the $S_0 \rightarrow {}^*S_1$ transition.[17, 18] The ground-state spectrum of the model ruthenium complex **8** is characterized by intense bands in the UV and visible regions. While the absorption observed around 300 nm corresponds to the bpy $\pi-\pi^*$ transition, the band at 450 nm is attributed to a metal-to-ligand charge-transfer band (MLCT).[8] The spectrum of dyad **6** (see supporting information) is virtually the sum of the individual spectra of **5** and **8**, as previously observed for different C_{60}-based ruthenium dyads.[9, 19] In line with the results of the electrochemical investigation, no bands attributable to any electronic interaction between the two ground-state chromophores were observed.

Steady-state luminescence: The emission spectrum of **5** (1.0×10^{-4} M) in methylcyclohexane at 77 K exhibits maxima at 703, 716, 725(sh), 739, 754, 783, and 796(sh) nm, and is a mirror image of the corresponding UV/visible absorption features. The fluorescence-quantum yield of photoexcited **5** ($\Phi_{rel} = 6.0 \times 10^{-4}$) indicates insignificant modification of the fullerene emission by the covalently linked androstane and bpy groups relative to pyrrolidine **7**. The emission bands of dyad **6**, recorded in a 1:1 toluene/CH_2Cl_2 mixture at 77 K ($\lambda_{exc} =$ 460 nm, $\lambda_{em}(max) = 630$ nm) are reasonably in line with those found for **8** and other polypyridineruthenium(II) complexes.[8] The emission spectrum, beginning at the long-wavelength tail of the excitation band, is a good mirror image of the excitation spectrum. This suggests that the luminescence undoubtedly originates from the MLCT excited state of the ruthenium moiety, and that other strongly fluorescent units are absent. Solvent polarity affected the luminescence intensity of dyad **6** (Table 2). Increasing the dielectric constant of the solvent led, in fact, to a drastic decrease of the luminescence quantum yield, relative to model **8** in CH_3CN (Figure 3). This solvent dependence is in sharp contrast to the luminescence behavior noticed for the previously mentioned flexible dyad,[10] in which the bipyridylruthenium(II) moiety is attached to the pyrrolidine ring through a triethylene glycol chain. This dyad shows an

Table 2. Photophysical properties of **8** and **6** in solvents of different polarity.

	Solvent	Luminescence intensity at 630 nm (77 K)	k_{et} [s^{-1}][a]
model **8**	CH_3CN	1	
dyad **6**	CH_2Cl_2/toluene	0.24	0.69×10^9
dyad **6**	CH_2Cl_2	0.11	2.1×10^9
dyad **6**	CH_3CN/toluene	0.029	3.5×10^9
dyad **6**	CH_3CN	0.021	5.1×10^9

[a] Evaluated from the lifetimes measured in transient absorption experiments at 25 °C.

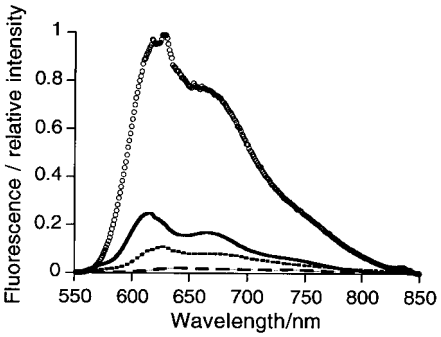

Figure 3. Emission spectrum (excitation at 460 nm) of dyad **6** in CH_3CN (dashed line), in CH_2Cl_2 (dotted line), in 1:1 toluene/CH_2Cl_2 (solid line), and **8** in CH_3CN (○) at 77 K. All samples were studied under identical conditions, therefore the relative intensities represent relative emission quantum yields.

efficient and solvent-independent deactivation of the MLCT state, suggesting the formation of an intramolecular exciplex.

The emission spectra of **6** and **8** were recorded for solutions with equal absorbance at the 460 nm excitation wavelength.[20] Accordingly, it is conceivable to attribute the decrease in luminescence intensity to intramolecular quenching of the ruthenium MLCT excited state by the fullerene moiety. Since the thermodynamic driving force $-\Delta G^{\circ}_{CS}$ for ET reactions is expected to become more exothermic with increasing solvent polarity, the current observation suggests a ET mechanism in photoexcited dyad **6** (vide infra).

It should be noted that the emission studies revealed no spectral evidence for any fullerene related fluorescence (700–800 nm) or phosphorescence (824 nm), regardless of the excitation wavelength. This can be rationalized in terms of the relative low quantum yields reported for these emissive processes (Φ_{FLU} ca. 6.0×10^{-4} and $\Phi_{PHO}\ll1.0\times10^{-4}$),[17] relative to the strong luminescence of the MLCT state.

*Pico- and nanosecond-resolved flash photolysis for the model compounds **5** and **7***: Differential absorption spectra of ligand **5** (2.0×10^{-5} M) in CH_2Cl_2, recorded after 532 nm excitation, indicate the immediate formation of the excited singlet state, with λ_{max} around 885 nm. The remarkable blue shift, relative to pristine C_{60} (920 nm), can be rationalized in terms of perturbation of the fullerene π system upon functionalization. The rate of intersystem crossing of the excited singlet state of **5** into the lower lying excited triplet state ($5.8\times10^{8}\,s^{-1}$) was followed by the decay of the absorption of the excited singlet at 885 nm and the simultaneous absorption growth of the excited triplet at 690 nm (Figure 4a).

Nanosecond-flash photolysis was carried out to complement the differential absorption changes involving the formation of the fullerene excited triplet state. Laser excitation of **5** (2.0×10^{-5} M) in CH_2Cl_2 resulted in differential absorption changes that display strong absorption maxima at 360 and 690 nm with a shoulder around 800 nm (Figure 5).

Similar results were obtained for derivative **7** both in the pico- and nanosecond timescale, thus showing that the bpy moiety does not affect the photophysical behavior of fullerene derivatives. Since the differential absorption changes between 300 and 850 nm are in excellent agreement with other monofunctionalized fullerene derivatives,[4, 17] the underlying process can be unambiguously ascribed to the formation of the excited triplet state of **5.**

*Pico- and nanosecond-resolved flash photolysis for dyad **6** and model compound **8**:* The solvent dependence of the luminescence of **6** was investigated by time-resolved photolysis, carried out in solvents of different polarity. Figure 4b shows differential absorption changes of **6** at various time delays (see Figure caption) following picosecond excitation in 1:1 toluene/CH_2Cl_2. Emission of the MLCT excited state causes the immediate ground-state bleaching in the displayed wavelength region (Figure 4b,c). However, the lifetime thereof is distinctly shortened relative to that recorded for model compound **8** and for other polypyridineruthenium(II) complexes.[8] While the excited state of **8** is essentially stable on the picosecond time scale and recovers to the ground state

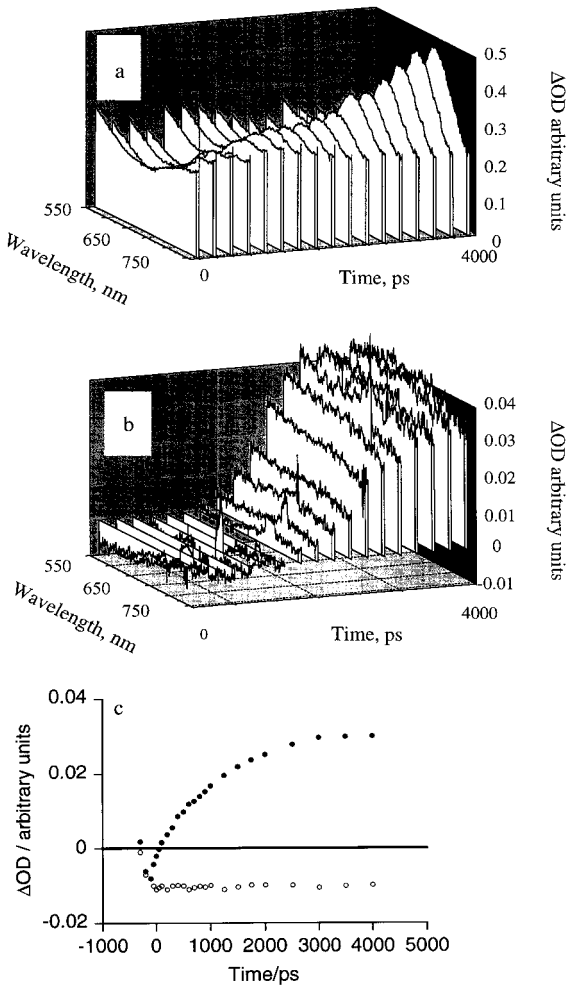

Figure 4. Time-resolved difference absorption spectra of a) **5** (2.0×10^{-5} M) in 1:1 toluene/ CH_2Cl_2 solution, and b) **6** (2.0×10^{-5} M) in CH_2Cl_2 solution 0, 50, 100, 150, 200, 300, 400, 500, 750, 1000, 1250, 1500, 2000, 2500, 3000, 3500, 4000, ps after excitation with a 18 ps laser pulse at 532 nm. c) Time absorption profiles recorded at 600 nm for **8** (○) in CH_3CN and **6** (●) in toluene/CH_2Cl_2 at room temperature.

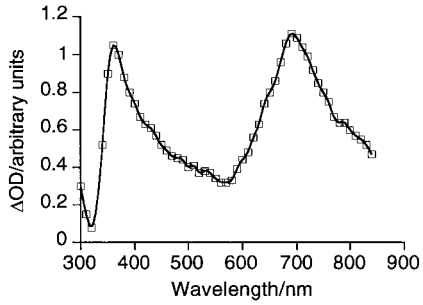

Figure 5. Differential absorption spectrum obtained upon flash photolysis of **5** (2.0×10^{-5} M) in CH_2Cl_2 with a 8 ns laser pulse at 337 nm.

with $\tau_{1/2}=150$ ns, the $^*Ru^{2+}$ related emission in dyad **6** transforms into a broad-absorbing species with $\tau_{1/2}=1.0$ ns (Figure 4b). The broad absorption features, recorded 4 ns after the pulse, are clearly different from the fullerene excited triplet state, which has a sharp $^*T_1\rightarrow{}^*T_n$ maximum around 690 nm. Accordingly, those features are tentatively interpreted in terms of the CS state $Ru^{3+}-C_{60}^{\bullet-}$.

0947-6539/98/0410-1996 $ 17.50+.50/0 *Chem. Eur. J.* **1998**, *4*, No. 10

In analogy to the luminescence quenching, the solvent polarity has a significant impact on the kinetics of the absorption growth. In particular, going from toluene/CH_2Cl_2 to CH_3CN enhanced the quenching rate in dyad **6** from $6.9 \times 10^8\ s^{-1}$ (toluene/CH_2Cl_2) to $2.1 \times 10^9\ s^{-1}$ (CH_2Cl_2) and $5.1 \times 10^9\ s^{-1}$ (CH_3CN). This trend correlates well with previous observations on electron-transfer reactions in D–A dyads[21] and corroborates our hypothesis of an intramolecular electron-transfer process from the ruthenium MLCT excited state to the fullerene moiety.

Corresponding photolytic studies in the nanosecond time regime have been performed to characterize the previously mentioned broad-absorbing species. Photolysis of dyad **6** in CH_2Cl_2 showed two relaxation processes (Figure 6a). The

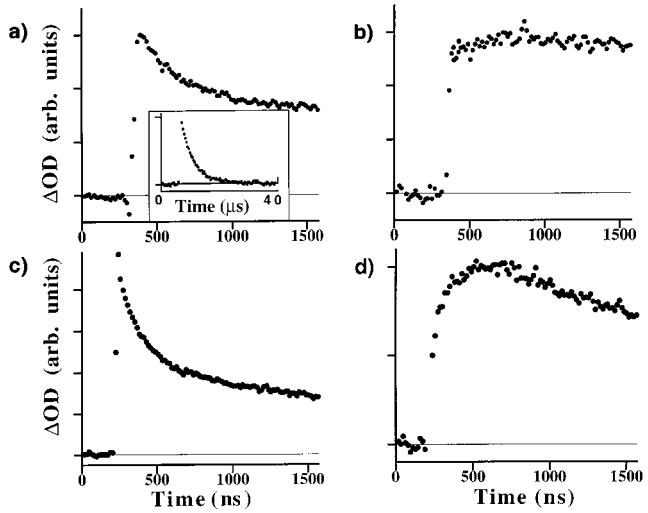

Figure 6. Time profiles of absorption following 337 nm flash photolysis of **6** (2.0×10^{-5} M) of a) Ru^{3+}–$C_{60}^{\bullet-}$ recorded at 390 nm in CH_2Cl_2, b) (Ru^{2+}–$^3C_{60}$) recorded at 690 nm in CH_2Cl_2, c) Ru^{3+}–$C_{60}^{\bullet-}$ recorded at 390 nm in CH_3CN, and d) (Ru^{2+}–$^3C_{60}$) recorded at 690 nm in CH_3CN. Inset in a) shows extended time scale at 390 nm.

faster process was an absorbance decay of the initially formed species that occurred with $\tau_{1/2} = 210$ ns. The slower process was a monoexponential recovery of the ground-state absorption with a half life of 10 μs (see inset to Figure 6a). The differential changes, recorded immediately after the excitation (ca. 50 ns) closely resemble those resulting from the absorption growth process observed during picosecond photolysis (4 ns, Figure 4b). In particular, this short-lived transient species displays a series of maxima at 390, 500, 570, and 640 nm (Figure 7a).

More importantly, a well-resolved near-IR absorption band with λ_{max} at 1040 nm, resembling the radiolytically reduced fullerene moiety (vide infra), reveals unambiguous evidence for the fullerene radical anion (Figure 7c). This substantiates the hypothesis that a CS state (Ru^{3+}–$C_{60}^{\bullet-}$, $\tau_{1/2} = 210$ ns in CH_2Cl_2) in dyad **6**, evolves from intramolecular oxidative quenching of the MLCT excited state.

Absorption features of the long-lived component (Figure 7b), recorded after the completion of the initial relaxation process (ca. 2 μs after the excitation) are remarkably different from those of the short-lived transient. Strong transition

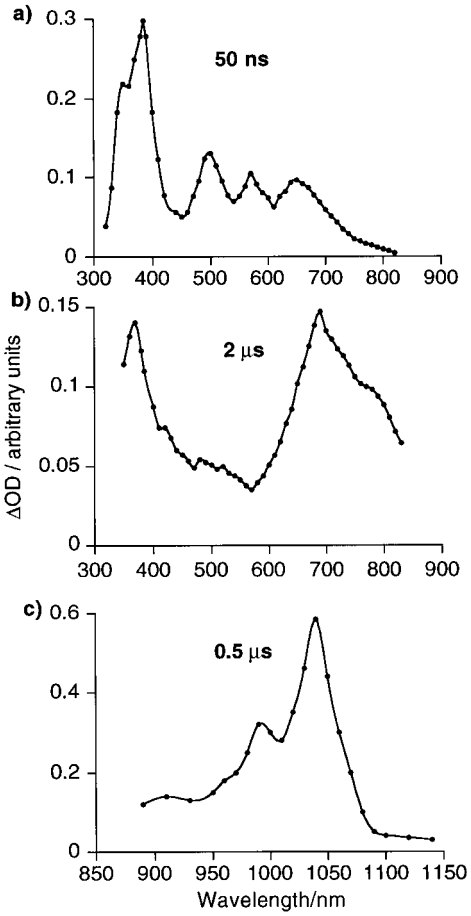

Figure 7. Differential absorption spectra obtained upon flash photolysis of **6** (2.0×10^{-5} M) in toluene/CH_2Cl_2 (1:1 v/v) with a 8 ns laser pulse at 337 nm. a) UV/Vis part recorded 50 ns after excitation; b) UV/Vis part recorded 2 μs after excitation; c) near-IR part recorded 0.5 μs after excitation.

bands at 360 and 690 nm with a well-pronounced shoulder around 800 nm correspond to the excited triplet states of the fullerene core as found for model compounds **7** and ligand **5** (Figure 5).

It should be noted, however, that both chromophores in dyad **6** have strong and overlapping absorption features in the UV/visible region. Consequently, direct excitation of the ruthenium antenna competes with light absorption by the fullerene core. This prompted us to investigate derivatives **5** and **7** in various solvents using different excitation wavelengths (308, 337, 355, and 532 nm). Indeed, after correction for the respective ground-state absorptions, **5** and **7** afforded similar triplet yields to **6**. In addition, Figure 6b demonstrates that the rapid growth of the $^*T_1 \rightarrow {}^*T_n$ absorption in CH_2Cl_2 is kinetically independent on the decay of the CS ion pair absorption at 390 nm (Figure 6a, ca. 1 μs). This leads to the conclusion that the photoexcited fullerene in dyad **6** is formed exclusively by intersystem crossing from the singlet state, which in turn is formed by direct excitation of the C_{60} chromophore.

In contrast to the results in CH_2Cl_2, the kinetics of growth of the $^*T_1 \rightarrow {}^*T_n$ absorption in CH_3CN reveals a two-step formation process (Figure 6d). The rise of the fast component is virtually completed with the instrument response and presumably involves direct excitation of the fullerene core.

The secondary contribution of the absorption growth is, nevertheless, kinetically linked to the decay of the CS ion pair absorption at 390 nm (Ru^{3+}–$C_{60}^{\bullet-}$, Figure 6c). They follow similar kinetics with $\tau_{1/2}$ about 100 ns. This would signify that the CS state in CH_3CN decays through the energetically lower lying triplet excited state to regenerate the ground state, rather than a direct recombination to the latter. The Ru^{2+}–$^3C_{60}$ state, derived from the two pathways, is produced with an overall quantum yield of essentially unity.[22]

The dielectric continuum model[23] yields a ΔG°_{CS} value of -0.24 eV for CH_3CN, that is, the regeneration of the excited ruthenium state from the CS state is endergonic. Accordingly, occurrence of charge recombination to ^{3}MLCT excited state is improbable, and back electron transfer proceeds via the fullerene excited triplet state ($E_{0\text{-}0} = 1.50$ eV). On the other hand, in CH_2Cl_2 the energy difference between the two states is very small (-0.02 eV). This suggests that back electron transfer to the ruthenium ^{3}MLCT excited state is favored relative to the CH_3CN case. In CH_3CN the above mentioned two-step decay process could be interpreted, within the Marcus theory, in terms of the high exergonicity of the direct formation of the ground state. The different routes for back electron transfer in **6** are summarized in the energy diagrams reported in Scheme 3.

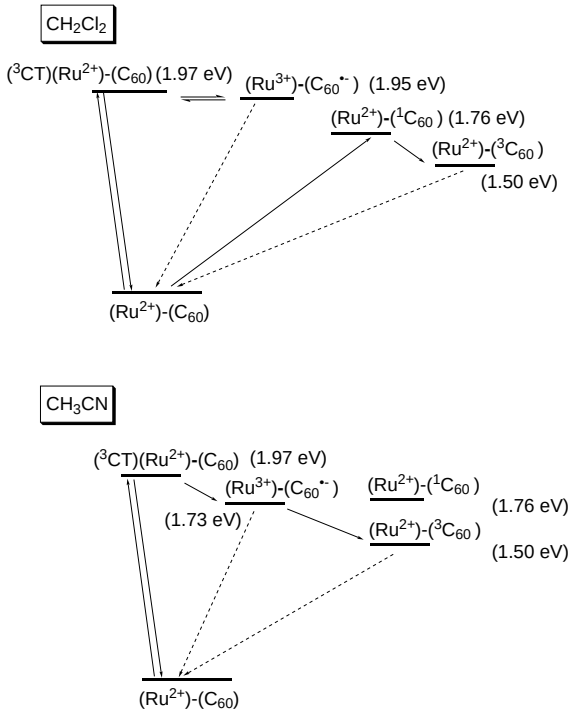

Scheme 3. Energy scheme for the excited states of **6** in CH_2Cl_2 and CH_3CN (see text and ref. [23]).

Pulse radiolysis: In order to further confirm the generation of the reduced fullerene moiety upon photolysis of dyad **6**, pulse irradiation was carried out. Radical anions of fullerenes can be studied by radiation-induced reduction of fullerenes in N_2-saturated 2-propanol.[24] The reducing species generated under those conditions are the solvated electron and the radical formed by hydrogen abstraction from 2-propanol, namely $(CH_3)_2\dot{C}(OH)$. Reduction of **6** took place with rate constants of $4.6 \times 10^{10}\,M^{-1}\,s^{-1}$ and $8.2 \times 10^{8}\,M^{-1}\,s^{-1}$ for the solvated electron and $(CH_3)_2\dot{C}(OH)$ radicals, respectively. The resulting absorption maximum at 1045 nm (indicative of $C_{60}^{\bullet-}$) is in good agreement with the one observed in the photoinduced intramolecular electron transfer from the MLCT excited states of the ruthenium moiety to the fullerene ground state (Figure 7c). This similarity corroborates the successful generation of the CS state (Ru^{3+}–$C_{60}^{\bullet-}$) in photoexcited dyad **6**.

However, the CS state of dyad **6** surprisingly lacks direct spectral evidence for the reduced fullerene moiety (e.g., ground-state bleaching at 330 nm and a broad transition band at 420 nm) or the oxidized ruthenium chromophore (e.g., ground-state bleaching around 450 nm). Thus, comparison between the data obtained upon photolysis of dyad **6** and pulse radiolysis of the individual model compounds **5** and **8** was helpful in the identification of the transient products.

Under reductive conditions, pulse irradiation of ligand **5** (2×10^{-5} M) in a toluene/2-propanol/acetone mixture (1:1:1 v/v) resulted in the formation of distinct and characteristic absorptions throughout the UV/visible and near-IR regions. The UV/visible part is shown in Figure 8a with a maximum

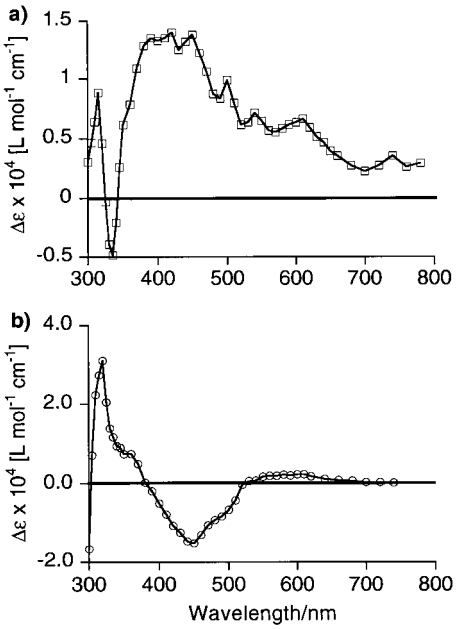

Figure 8. a) Radiolytic reduction of **5**: transient absorption spectrum (□) of the C_{60} radical anion obtained upon pulse radiolysis in N_2-saturated toluene/2-propanol/acetone mixture (1:1:1 v/v). b) Radiolytic oxidation of **8**: transient absorption spectrum (○) of Ru^{III} obtained upon pulse radiolysis in N_2O-saturated aqueous solution containing 0.1 M HCl.

around 420 nm ($\Delta\varepsilon = 14000\,M^{-1}\,cm^{-1}$ at 420 nm).[25] These features are ascribed to the C_{60} radical anion formed in the reaction shown in Equation (1).

$$(C_{60})\text{–}R + (CH_3)_2\dot{C}(OH) \longrightarrow (C_{60}^{\bullet-})\text{–}R + (CH_3)_2CO + H^+ \quad (1)$$

On the other hand, radiolytic oxidation of water-soluble substrates such as **8** can be conveniently studied in N_2O

0947-6539/98/0410-1998 $ 17.50+.50/0 *Chem. Eur. J.* **1998**, *4*, No. 10

saturated solution containing 0.1M HCl; this leads to the formation of the well characterized $Cl_2^{\bullet-}$ (λ_{max} at 340 nm). Addition of variable amounts of **8** resulted in an accelerated decay of the $Cl_2^{\bullet-}$ absorption, indicating oxidation of the ruthenium(II) complex [Eq. (2)] with a rate constant of $1.1 \times 10^9\,M^{-1}s^{-1}$. The resulting absorption changes (20 μs after the pulse) showed bleaching of the starting material around 450 nm ($\Delta\varepsilon = 13000\,M^{-1}cm^{-1}$ at 450 nm) and formation of weak absorption around 550 nm (Figure 8b).

$$Cl_2^{\bullet-} + [Ru(bpy)_2(bpy{-}CO_2R)]^{2+} \longrightarrow 2\,Cl^- + [Ru(bpy)_2(bpy{-}CO_2R)]^{3+} \quad (2)$$

Determination of the differential absorption changes, which evolve from reduction and oxidation of the two individual chromophores, permits the interpretation of the spectral features (UV/visible range) found for the CS state of dyad **6** (Figure 7a). The spectral features of $Ru^{3+}{-}C_{60}^{\bullet-}$ are essentially a superimposition of the absorption observed for the reduced fullerene moiety ($C_{60}^{\bullet-}$, Figure 8a) and the oxidized ruthenium complex (Ru^{3+}, Figure 8b). The strong transition band of the reduced fullerene moiety (around 420 nm) masks the ruthenium related bleaching (around 440 nm), and bleaching of ground-state fullerene (around 335 nm) is compensated by the sharp absorption of the ruthenium(III) complex in this range.

Conclusion

In this paper we have described the synthesis, electrochemistry, and photophysical behavior of a $[Ru(bpy)_3^{2+}]{-}C_{60}$ dyad in which the spacer between the metal complex and the C_{60} is a rigid androstane moiety. UV/visible absorption spectroscopy and electrochemical investigations suggest the absence of any ground-state interaction between the $[Ru(bpy)_3^{2+}]$ and fullerene chromophores. This is in line with previous studies performed on a similar dyad in which the C_{60} and ruthenium chromophores are linked through a flexible triethylene glycol spacer. Steady-state fluorescence of dyad **6** showed a rapid, solvent-dependent, intramolecular quenching of the ruthenium MLCT excited state. Time-resolved flash photolysis (pico- and nanosecond) in CH_2Cl_2 and CH_3CN revealed characteristic differential absorption changes throughout the UV/visible and near-IR range that have been ascribed to the formation of the CS state $Ru^{3+}{-}C_{60}^{\bullet-}$, with $\tau_{1/2} = 210$ ns in CH_2Cl_2 and $\tau_{1/2} = 100$ ns in CH_3CN. It is worth noting that in polar solvents the use of a rigid spacer instead of a flexible chain allows efficient charge separation. The flexible dyad may adopt a folded conformation in solution with the ruthenium and C_{60} chromophores in close proximity, thus promoting fast charge recombination. The most interesting result concerning the photophysical properties of dyad **6** is that back electron-transfer reaction products depend on the solvent used. While the $Ru^{3+}{-}C_{60}^{\bullet-}$ pair decays in CH_3CN through the formation of the lower lying triplet excited state of C_{60}, regeneration of the MLCT excited state has been suggested to be the predominant deactivation route in CH_2Cl_2.

In order to increase the efficiency of the formation of the CS state and lifetime thereof we are currently working on the design and preparation of novel systems containing multinuclear metal centers and C_{60}-based triads.

Experimental Section

Instrumentation: Details regarding instrumentation used in this paper have been described elsewhere.[4c, 13, 26] MM2 and PM3 calculations were performed using the SPARTAN 4 program running on a IBM/6000 workstation.

Materials: C_{60} was purchased from Bucky USA (99.5 %). All other reagents were used as purchased from Fluka and Aldrich. 5-Methyl-2,2′-bipyridine,[27] 2,2′-bipyridine-5-carboxylic acid,[28] *cis*-bis(2,2′-bipyridine-*N*,*N*′)-dichlororuthenium(II) dihydrate,[29] and *N*-methylfulleropyrrolidine[7a] were prepared as described in the literature. All solvents were distilled prior to use. Methylcyclohexane, toluene, dichoromethane, acetonitrile, acetone, and 2-propanol employed for UV/visible, fluorescence, phosphorescence, pico- and nanosecond flash photolysis, and pulse radiolysis measurements were commercial spectrophotometric grade solvents that were carefully deoxygenated prior to use.

Abbreviations used: bpy = 2,2′-bipyridine; DCE = 1,2-dichloroethane; THF = tetrahydrofuran; DCC = dicyclohexylcarbodiimide; DMAP = 4-dimethylaminopyridine; TBAH = tetrabutylammonium hexafluorophosphate.

^1H and ^{13}C NMR data of derivatives **4**–**6** and **8**, ^1H and ^{13}C NMR spectra of dyad **6**, UV/visible spectra of derivatives **5**, **6**, and **8**, and CV curves of substrates **4**, **5**, **7**, and **8** are available as supporting information.

17β-(ol-2,2′-bipyridylcarboxylate)-5α-androstan-3-one (**4**): DMAP (34 mg, 0.28 mmol) and DCC (120 mg, 0.58 mmol) were added to a suspension of **2** (0.11 g, 0.55 mmol) in CH_2Cl_2 (3 mL), and the mixture was stirred at room temperature for 20 minutes. A solution of **3** (145 mg, 0.5 mmol) in CH_2Cl_2 (2 mL) was added, and the mixture stirred for a further 20 h at room temperature. The solvent was removed under reduced pressure, and the solid residue was purified by flash column chromatography (SiO_2, eluant toluene/AcOEt 9:1, then 8:2) affording **4** (153 mg, 65 %). M.p. 226–230 °C; IR (KBr): $\tilde{\nu} = 2933, 1715, 1594, 1282, 762\ cm^{-1}$; $C_{30}H_{36}N_2O_3$ (472.3): calcd C 76.24, H 7.68, N 5.93; found C 76.42, H 8.01, N 5.55.

***N*-Methyl-3,4-fulleropyrrolidine-2-spiro-17′β-(ol-2,2′-bipyridylcarboxylate)-5′α-androstanyl** (**5**): A solution of C_{60} (112 mg, 0.16 mmol), **4** (70 mg, 0.15 mmol), and *N*-methylglycine (47 mg, 0.52 mmol) in toluene (100 mL) was heated to reflux for 2.5 h. The solvent was evaporated under reduced pressure, and the crude product purified by flash column chromatography (SiO_2). Elution with toluene/AcOEt 95:5 and then 9:1 gave **5** (34 mg, 19 %) along with unreacted C_{60} (73 mg, 65 %). IR (KBr): $\tilde{\nu} = 2923, 1721, 1590, 1458, 1279, 1116, 760, 528\ cm^{-1}$; UV/Vis ($CH_2Cl_2$): $\lambda\ (\varepsilon) = 253\ (111000), 315\ (48400), 431$ nm (3720); MS (MALDI): *m/z* : 1218 $[M+H]^+$; $C_{92}H_{39}N_3O_2$ (1217.3): calcd C 90.70, H 3.23, N 3.45; found C 88.09, H 3.36, N 3.19.

[Ru(bpy)$_2$(5)](PF$_6$)$_2$ (**6**): A solution of **5** (31 mg, 0.025 mmol), $Ru(bpy)_2Cl_2 \cdot 2H_2O$[29] (14 mg, 0.027 mmol), and NH_4PF_6 (37 mg, 0.23 mmol) in DCE (8 mL) was heated to reflux for 9 h under a nitrogen atmosphere and in the dark. The reaction was monitored by TLC (toluene/AcOEt 6:4) through observation of the disappearence of **5**. After filtration, the solution was concentrated at reduced pressure, and the residue washed with toluene, MeOH, and water. The product was then dissolved in THF, filtered, and, after evaporation of the solvent, dried in vacuo affording **6** (20 mg, 41 %) as a brownish solid. IR (KBr): $\tilde{\nu} = 2925, 1726, 1464, 1447, 1298, 1143, 842, 762, 558, 528\ cm^{-1}$; UV/Vis ($CH_2Cl_2$): $\lambda\ (\varepsilon) = 255\ (103900), 287\ (103300), 432\ (11900), 447$ nm (11100); MS (APCI): *m/z* : 815 $[(M-2PF_6)/2]$; $C_{112}H_{54}N_7O_2F_{12}P_2Ru$ (1920.6): calcd C 70.0, H 2.83, N 5.10; found: C 64.74, H 2.86, N 4.87. Although the value for carbon is low, it is not unusual for fullerene derivatives.[30]

[Ru(bpy)$_2$(4)](PF$_6$)$_2$ (**8**): A solution of **4** (25 mg, 0.053 mmol), $Ru(bpy)_2Cl_2 \cdot 2H_2O$ (32 mg, 0.062 mmol), and NH_4PF_6 (90 mg, 0.55 mmol) in DCE (10 mL) was heated to reflux for 7 h under a nitrogen atmosphere. The solvent was removed under reduced pressure, and the solid residue purified by flash column chromatography (neutral Alumina, eluant

CH_3CN/toluene 3:1) affording **8** (16 mg, 25 %) as an orange compound. IR (KBr): $\tilde{\nu} = 2931$, 1710, 1466, 1447, 1299, 841, 559 cm^{-1}; UV/Vis (CH_2Cl_2): λ (ε) = 251 (17700), 288 (55000), 449 nm (7400); MS (MALDI): *m/z* : 1032 $[M - PF_6+H]^+$, 887 $[M - 2PF_6+H]^+$; MS (APCI): *m/z* : $[C_{50}H_{52}N_6O_3Ru]^{2+} = 443$ [*M*/2]; $C_{50}H_{52}N_6O_3P_2F_{12}Ru$ (1175.9): calcd C 51.07, H 4.46, N 7.15; found C 50.22, H 4.30, N 6.81.

Acknowledgments: We thank Dr. R. Seraglia (CNR-Padova) for MALDI-MS data. We are indebted to Prof. M. Prato for a critical reading of the manuscript. Part of this work was supported by the Office of Basic Energy Sciences of the U.S. Department of Energy (contribution No. 4015 from the Notre Dame Radiation Laboratory), C.N.R. (*Progetto Strategico Materiali Innovativi*), MURST, and University of Bologna (funds for selected topics). D.G. and M.M. thank NATO Collaborative Research Grants Program for a travel grant (grant No. CRG960099).

Received: November 12, 1997
Revised version: April 16, 1998 [F888]

[1] a) *The Photosynthetic Reaction Center* (Eds.: J. Deisenhofer, J. R. Norris), Academic Press, San Diego, **1993**; b) *Photoinduced Electron Transfer* (Eds.: M. A. Fox, M. Chanon), Elsevier, Amsterdam, **1988**; c) *Molecular Electronic Devices* (Eds.: F. L. Carter, R. E. Siatkowski, H. Wohltjen), Norte-Holland, Amsterdam, **1988**; d) *Molecular Electronics Science and Technology* (Ed.: A. Aviram), American Institute of Physics, New York, **1992**; e) V. Balzani, F. Scandola, *Supramolecular Photochemistry*, Ellis Horwood, London, **1991**; f) D. Gust, T. A. Moore, in *Photoinduced Electron Transfer III* (Ed.: J. Mattay), Springer, Berlin, **1991**; g) *Biological Applications of Photochemical Switches* (Ed.: H. Morrison), Bioorganic Photochemistry, Wiley, New York, **1993**.

[2] M. R. Wasielewski, *Chem. Rev.* **1992**, *92*, 435.

[3] a) N. S. Sariciftci, L. Smilowitz, A. J. Heeger, F. Wudl, *Science* **1992**, *258*, 1474; b) R. M. Williams, J. W. Verhoeven, *Chem. Phys. Lett.* **1992**, *194*, 446; c) Y. Wang, *Nature* **1992**, *356*, 585; d) J. W. Arbogast, A. P. Darmanian, C. S. Foote, Y. Rubin, F. Diederich, M. M. Alvarez, S. J. Anz, R. L. Whetten, *J. Phys. Chem.* **1991**, *95*, 11.

[4] a) H. Imahori, Y. Sakata, *Adv. Mater.* **1997**, *9*, 537, and references therein; b) P. A. Liddell, D. Kuciauskas, J. P. Sumida, B. Nash, D. Nguyen, A. L. Moore, T. A. Moore, D. Gust, *J. Am. Chem. Soc.* **1997**, *119*, 1400; c) D. M. Guldi, M. Maggini, G. Scorrano, M. Prato, *J. Am. Chem. Soc.* **1997**, *119*, 974; d) Y. Sun, T. Drovetskaya, R. D. Bolskar, R. Bau, P. D. W. Boyd, C. A. Reed, *J. Org. Chem.* **1997**, *62*, 3642; e) P. S. Baran, R. R. Monaco, A. U. Khan, D. I. Schuster, S. R. Wilson, *J. Am. Chem. Soc.* **1997**, *119*, 8363; f) H. Imahori, K. Yamada, M. Hasegawa, S. Taniguchi, T. Okada, Y. Sakata, *Angew. Chem.* **1997**, *109*, 2740; *Angew. Chem. Int. Ed. Engl.* **1997**, *36*, 2626; g) N. Armaroli, F. Diederich, C. O. Dietrich-Buchecker, L. Flamigni, G. Marconi, J.-F. Nierengarten, J.-P. Sauvage *Chem. Eur. J.* **1998**, *4*, 406.

[5] A. Hirsch, *The Chemistry of the Fullerenes*, Thieme, Stuttgart, **1994**.

[6] M. Prato, *J. Mater. Chem.* **1997**, *7*, 1097.

[7] a) M. Maggini, G. Scorrano, M. Prato, *J. Am. Chem. Soc.* **1993**, *115*, 9798; b) X. Zhang, M. Willems, C. S. Foote, *Tetrahedron Lett.* **1993**, *34*, 8187.

[8] a) *Photochemistry and Photophysics of Coordination Compounds* (Eds.: H. Yersin, A. Vogler), Springer, Berlin, **1987**; b) A. Juris, V. Balzani, F. Barigelletti, S. Campagna, P. Belser, A. Zelewsky, *Coord. Chem. Rev.* **1988**, *84*, 85; c) J. P. Collin, S. Guillerez, J. P. Sauvage, F. Barigelletti, L. Flamigni, L. De Cola, V. Balzani, *Coord. Chem. Rev.* **1991**, *111*, 291; d) *Charge Transfer Photochemistry* (Eds.: O. Horvath, K. L. Stevenson), VCH, Weinheim, **1993**; e) V. Balzani, A. Juris, M. Venturi, S. Campagna, S. Serroni, *Chem. Rev.* **1996**, *96*, 759.

[9] M. Maggini, A. Donò, G. Scorrano, M. Prato, *J. Chem. Soc. Chem. Commun.* **1995**, 845.

[10] N. S. Sariciftci, F. Wudl, A. J. Heeger, M. Maggini, G. Scorrano, M. Prato, J. Bourassa, P. C. Ford, *Chem. Phys. Lett.* **1995**, *247*, 210.

[11] As a matter of fact, $[Ru(bpy)_3]^{2+}$ octahedral complexes are chiral, so four diastereoisomers for dyad **6** are, in principle, possible.

[12] M. G. Teixeira, S. Roffia, C. A. Bignozzi, C. Paradisi, F. Paolucci, *J. Electroanal. Chem.* **1993**, *345*, 243.

[13] F. Paolucci, M. Marcaccio, S. Roffia, G. Orlandi, F. Zerbetto, M. Prato, M. Maggini, G. Scorrano, *J. Am. Chem. Soc.* **1995**, *117*, 6572.

[14] The CV curve for fulleropyrrolidine **7** resembles that already reported in a different medium (see M. Prato, M. Maggini, C. Giacometti, G. Scorrano, G. Sandonà, G. Farnia, *Tetrahedron* **1996**, *52*, 5221). In order to ensure identical scaling, the CV for **7** was recorded under the same conditions to those used for compound **8** (Scheme 2).

[15] S. Roffia, M. Marcaccio, C. Paradisi, F. Paolucci, V. Balzani, G. Denti, S. Serroni, S. Campagna, *Inorg. Chem.* **1993**, *32*, 3003.

[16] C. Foote, *Top. Curr. Chem.* **1994**, *169*, 347.

[17] R. M. Williams, J. M. Zvier, J. W. Verhoeven, *J. Am. Chem. Soc.* **1995**, *117*, 4093.

[18] D. Zhou, L. Gan, H. Tan, C. Luo, C. Huang, G. Yao, B. Zhang, *J. Photochem. Photobiol. A: Chemistry* **1996**, *99*, 37.

[19] D. Armspach, E. C. Constable, F. Diederich, C. E. Housecroft, J.-F. Nierengarten, *Chem. Commun.* **1996**, 2009.

[20] For derivative **6**, part of the exciting light is absorbed by the fullerene core. Although this effect has been taken into account, the luminescence intensity of **6** is lower than that of **8**.

[21] a) M. N. Paddon-Row, *Acc. Chem. Res.* **1994**, *27*, 18; b) R. N. Williams, M. Koeberg, J. M. Lawson, Y. Rubin, M. N. Paddon-Row, J. W. Verhoeven, *J. Org. Chem.* **1996**, *61*, 5055.

[22] The quantum yield of the fullerene triplet excited state in CH_3CN was confirmed to be $\Phi = 0.95$ and is identical to that found for the fullerene model by triplet–triplet energy transfer method with a squarine dye as energy acceptor. In CH_2Cl_2 the quantum yield of the triplet state is $\Phi = 0.64$, which corresponds to the relative ground-state absorption of the fullerene moiety at the excitation wavelength.

[23] The solvent effect on the energy of the CS state was estimated with the dielectric continuum model. This model accounts for two spherical ions with radii r_A (C_{60}) and r_D $[Ru(bpy)_3]^{2+}$ separated by a distance r_{DA} immersed in a dielectric continuum with relative permittivity ε ($\varepsilon_{acetonitrile} = 35.94$, $\varepsilon_{dichloromethane} = 8.93$). $r_A = 4.4$ Å, $r_D = 4.1$ Å, and $r_{DA} = 20$ Å based on an averaged edge-to-edge distance of 11.5 Å for the two diastereoisomers (see text). These data were obtained from PM3 semiempirical calculations. The standard potentials for oxidation [$Ru^{II/III}$] and reduction (C_{60}/C_{60}^-) processes in CH_3CN reported in Table 1, and an E_{0-0} value of 1.97 eV relative to ^{3}MLCT of $[Ru(bpy)_3]^{2+}$ state were used in the calculations. For CH_2Cl_2 a correction to the above standard potentials was performed as described in the literature. a) A. Z. Weller, *Phys. Chem.* **1982**, *93*, 1982; b) H. Imahori, K. Hagiwara, M. Aoki, T. Akiyama, S. Taniguchi, T. Okada, M. Shirakawa, Y. Sakata, *J. Am. Chem. Soc.* **1996**, *118*, 11771; c) S. I. van Dijk, C. P. Groen, F. Hartl, A. Brouwer, J. W. Verhoeven, *J. Am. Chem. Soc.* **1996**, *118*, 8425.

[24] a) D. M. Guldi, *J. Phys. Chem. A* **1997**, *101*, 3895; b) D. M. Guldi, H. Hungerbühler, E. Janata, K.-D. Asmus, *J. Phys. Chem.* **1993**, *97*, 11258.

[25] Q. G. Mulazzani, M. Venturi, F. Bolletta, V. Balzani, *Inorg. Chim. Acta* **1986**, *113*, L1.

[26] A. Bianco, M. Maggini, G. Scorrano, C. Toniolo, G. Marconi, C. Villani, M. Prato, *J. Am. Chem. Soc.* **1996**, *118*, 4072.

[27] F. Kröhnke, *Angew. Chem.* **1963**, *75*, 181; *Angew. Chem. Int. Ed. Engl.* **1963**, *2*, 225.

[28] N. J. Neil, B. J. Beattie, *J. Med. Chem.* **1993**, *36*, 3853.

[29] P. Belser, A. von Zelewsky, *Helv. Chim. Acta* **1980**, *63*, 1675.

[30] J. C. Hummelen, B. Knight, J. Pavlovich, R. Gonzàlez, F. Wudl, *Science* **1995**, *269*, 1554.